Human Molecular Genetics, 2013, Vol. 22, No. 18 **3609–3623**
doi:10.1093/hmg/ddt212
Advance Access published on May 10, 2013

GATA3 controls the specification of prosensory domain and neuronal survival in the mouse cochlea

Xiong-jian Luo[1,2], Min Deng[2], Xiaoling Xie[2], Liang Huang[3,4,5], Hui Wang[6], Lichun Jiang[6], Guoqing Liang[1], Fang Hu[7], Roger Tieu[2], Rui Chen[6] and Lin Gan[1,2,*]

[1]College of Life and Environmental Sciences, Hangzhou Normal University, Hangzhou, Zhejiang 310036, China [2]Flaum Eye Institute and Department of Ophthalmology, University of Rochester, Rochester, NY 14642, USA [3]Nanchang University, Nanchang, Jiangxi 330006, China [4]Jiangxi Provincial People's Hospital, Nanchang, Jiangxi 330006, China [5]Gannan Medical University, Ganzhou, Jiangxi 341000, China [6]Department of Molecular and Human Genetics, Baylor College of Medicine, Houston, TX 77030, USA and [7]Affiliated Eye Hospital of Nanchang University, Nanchang, Jiangxi 330006, China

Received December 18, 2012; Revised May 1, 2013; Accepted May 6, 2013

HDR syndrome (also known as Barakat syndrome) is a developmental disorder characterized by hypoparathyroidism, sensorineural deafness and renal disease. Although genetic mapping and subsequent functional studies indicate that *GATA3* haplo-insufficiency causes human HDR syndrome, the role of *Gata3* in sensorineural deafness and auditory system development is largely unknown. In this study, we show that *Gata3* is continuously expressed in the developing mouse inner ear. Conditional knockout of *Gata3* in the developing inner ear disrupts the morphogenesis of mouse inner ear, resulting in a disorganized and shortened cochlear duct with significant fewer hair cells and supporting cells. Loss of *Gata3* function leads to the failure in the specification of prosensory domain and subsequently, to increased cell death in the cochlear duct. Moreover, though the initial generation of cochleovestibular ganglion (CVG) cells is not affected in *Gata3*-null mice, spiral ganglion neurons (SGNs) are nearly depleted due to apoptosis. Our results demonstrate the essential role of *Gata3* in specifying the prosensory domain in the cochlea and in regulating the survival of SGNs, thus identifying a molecular mechanism underlying human HDR syndrome.

INTRODUCTION

In mammals, sound and balance perceptions are mediated by the inner ear, a complicated structure consisting of the cochlea and the vestibular systems. The core auditory component of the cochlea is the organ of Corti that contains the sensory hair cells and supporting cells. Mammalian cochlear hair cells come in two anatomically and functionally distinct types: the outer and inner hair cells (OHCs and IHCs). The IHCs detect the sound waves in the fluids of the cochlea and transform them into electrical signals that are then relayed via the auditory nerve (spiral ganglion) to the auditory brainstem and to the auditory cortex, whereas the OHCs are thought to modulate the sound wave by interacting with the mechanics of the cochlear partition.

During development, the highly specialized and complex inner ear structure is generated through precise genetic controls. Many genes that regulate the development of the inner ear have been identified (1). Among these genes, transcription factors, including *Atoh1* (encoding a basic helix-loop-helix family transcription factor) (2), *Sox2* (encoding a Sry-related HMG box transcription factor) (3), *Pax2* (encoding a paired box homeotic transcription factor) (4), and *Pou4f3* (encoding a POU-homeodomain transcription factor) (5,6) have been subjected to special attention since targeted mutagenesis of these genes causes severe developmental defects in the sensory organs of the inner ear. For example, *Sox2* is required for specifying the sensory precursors in the organ of Corti (3), whereas *Atoh1* is indispensable for the differentiation of precursors into hair cells (2,7). Similarly, transcription factors play crucial roles in the development of the inner ear neurons. The basic helix-loop-helix family transcription factor NEUROD is one of the earliest markers for cochleovestibular ganglion (CVG) and the loss of

*To whom correspondence should be addressed at: 601 Elmwood Ave, Box 659; Flaum Eye Institute and Department of Ophthalmology, University of Rochester, Rochester, NY 14642, USA. Tel: +1 5852731510; Fax: +1 5852762432; Email: lin_gan@urmc.rochester.edu

NeuroD leads to a rapid loss of neurons from the CVG after delamination, resulting in a loss of nearly all neurons at embryonic day (E) 13.5 in mice (8). Conversely, ectopic expression of *NeuroD* in *in vitro* inner ear explant culture is sufficient to transform non-sensory cells into neuronal cells (9). These results demonstrate the crucial roles of transcription factors in the inner ear development.

The evolutionarily conserved GATA family transcription factors are characterized by their ability to bind to a consensus DNA sequence 5′-(A/T)GATA(A/G)-3′ through their conserved zinc finger DNA-binding domains (10). Six GATA factors (GATA1-6) have been identified in vertebrates and are expressed in different tissues (10). Among them, GATA3 plays a pivotal role in hearing as haplo-insufficiency of *GATA3* causes human HDR syndrome (11), a developmental disease characterized by hypoparathyroidism (H), sensorineural deafness (D), and renal disease (R) (12). In the developing kidney, *Gata3* is necessary for the morphogenesis and guidance of the nephric duct (13). Recently, Grigorieva *et al*. (14) found that *Gata3*-deficient mice develop parathyroid abnormalities due to dysregulation of the parathyroid-specific transcription factor GCM2. Though these studies have revealed the role of the *GATA3* gene in the development and function of the parathyroid and the kidney (two organs that are affected by HDR syndrome), it is not known how GATA3 regulates auditory system development and function.

Previous studies show that *Gata3* is expressed in the inner ear and auditory neurons (15–25), and that targeted mutagenesis of *Gata3* affects the early morphogenesis of the ear (16). *Gata3*-null mutation causes early embryonic lethality around E12 (26), a stage with only limited inner ear morphogenesis. *Gata3*-deficient embryos partially rescued by L-phenylephrine remain defective in sensory organ morphogenesis. While in the drug rescued embryos, the vestibular sensory epithelium succeeded in producing a limited number of hair cells, no evidence for sensory differentiation is detected in the cochlear sensory epithelium (27). Here, to elucidate the precise role of *Gata3* in the development of inner ear sensory organs and neurons and in deafness diseases, we created a mouse conditional knockout allele of *Gata3* and used *Pax2-Cre* mice to delete *Gata3* specifically in the developing ear. We found that conditional knockout of *Gata3* causes severe inner ear defects. Compared with normal controls, *Gata3*-null mice have a dramatically shortened cochlea duct due to elevated apoptosis and very limited genesis of hair cells and supporting cells. Moreover, the loss of *Gata3* alters the expression pattern of genes in the cochlea during sensory organ formation. Furthermore, the spiral ganglion neurons (SGNs) were largely missing in *Gata3*-null mice. Our results demonstrated that *Gata3* plays an essential role in inner ear development by specifying the prosensory domain in the cochlea and controlling the survival of SGNs, and support the role of *Gata3* in HDR disease.

RESULTS

Expression of GATA3 in the developing mouse inner ear

The mammalian inner ear is a highly conserved structure with a total of six sensory organs (28). The five vestibular sensory organs include the three cristae at the bases of the corresponding anterior, lateral and posterior semicircular canals, and the utricular and saccular maculae located within the central vestibule. The sensory organ of hearing, the organ of Corti, is housed within the cochlea. All of these structures in the inner ear develop from an otic placode that invaginates to form the spherical otocyst by E9.5. The otocyst undergoes series of development, including regional specialization and complex morphological conversion to form the highly specialized inner ear that mediates hearing and balance (28,29).

To study the role of *Gata3* in the inner ear development, we first detailed the spatiotemporal expression pattern of *Gata3* in the developing mouse inner ear by anti-GATA3 immunohistochemistry. At E9.5, GATA3 is strongly expressed in the entire otocyst (Fig. 1A). At E10.5 and E11.5, GATA3 expression is confined to the dorsolateral and mid-ventral parts of the otocyst (Fig. 1B and C). At E12.5, GATA3 is broadly expressed in the cochlear duct and in selected CVG cells (Fig. 1D), and its expression persists in spiral ganglion cells and cochlea duct from E13.5 to E18.5 (Fig. 1E–H).

To assess further the expression pattern of GATA3 in developing ganglion cells, we co-labeled GATA3 with two CVG markers, NEUROD (8) and ISL1 (30). At E9.5, when neuroblasts begin to delaminate from the ventral region of the otocyst and form the CVG, GATA3 is expressed in a majority of the NEUROD+ cells (Fig. 1I). When the CVG structure becomes more defined at E10.5 to E12.5, GATA3 expression was detected in a proportion of NEUROD+ CVG (Fig. 1J–L). Co-immunostaining with a pan-CVG neuronal marker ISL1 also revealed GATA3 expression in a selective group of CVG neurons (Fig. 1M–P). Finally, we co-labeled GATA3 with TUJ1, a mature neural marker, and found that GATA3 is highly expressed in SGNs (Fig. 1Q–T). Taken together, these results indicate that GATA3 is continuously expressed throughout the development of the cochlea and spiral ganglion, suggesting the role of GATA3 in the inner ear development.

Inner ear-specific deletion of *Gata3* in mice

To investigate the role of *Gata3* in the inner ear development, we generated *Gata3* conditional knockout mice by flanking Exon 4 with loxP sequences (Fig. 2A and B). Since Exon 4 of *Gata*3 gene encodes the first zing finger motif important for DNA binding, removing this region created a non-functional protein and in addition, caused reading frame-shift and a premature termination codon in Exon 5. We used $Pax2^{cre}$ driver line, which express Cre recombinase in the developing otocyst (31), to conditionally inactivate *Gata3* in the developing inner ear. Compared with GATA3 nuclear expression seen in the otic epithelial cells of the wild-type control at E9.5, anti-GATA3 immunolabeling detected no specific, nuclear expression of GATA3 in the otocyst of *Gata3*-null mice (Fig. 2C–F). These results indicate that $Pax2^{cre}$ driver line efficiently deleted the $Gata3^{loxP}$ allele early during inner ear development. In addition, we noted that *Gata3*-null mice died shortly after birth, which is likely due to the dysfunction of the kidney in which $Pax2^{cre}$ also drives the expression of Cre recombinase. Finally, compared with wild-type mice, *Gata*3 heterozygous mice weighed significantly less than the wild-type controls from postnatal day 27 (Supplementary Material, Fig. S1), which may due to the abnormal function of the parathyroid in *Gata*3 heterozygous (14).

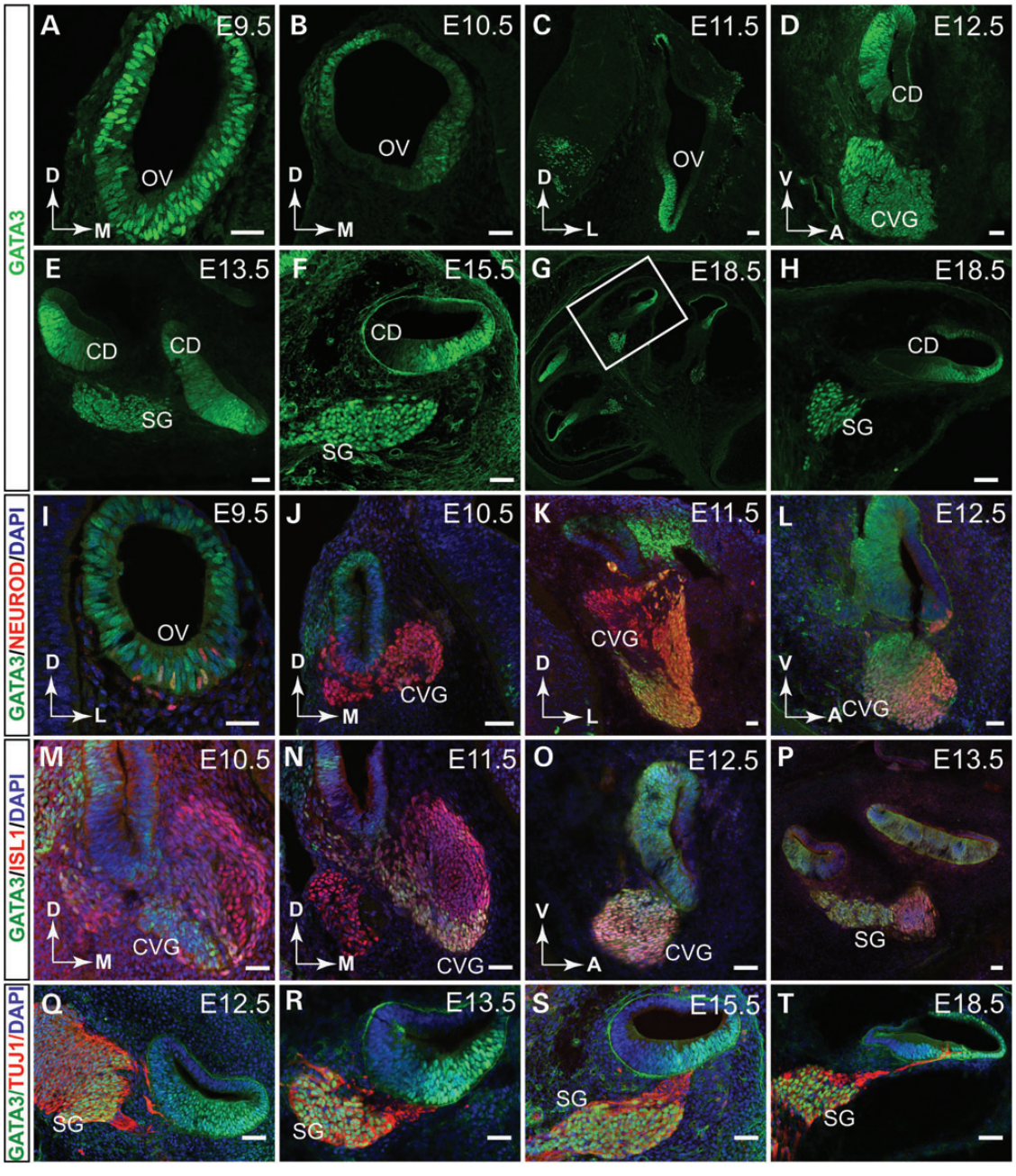

Figure 1. The expression of GATA3 in the developing mouse inner ear. (**A**) Immunolabeling on transverse sections through the otic vesicle reveals that GATA3 is expressed in the entire otocyst at E9.5. (**B** and **C**) The expression of GATA3 is detected in the dorsolateral and ventromedial domains of the otocyst at E10.5 and E11.5. (**D**) At E12.5, GATA3 is widely expressed in the ventral cochlear duct and partially in the CVG. (**E**–**H**) From E13.5, GATA3 is strongly expressed in the SG and the cochlear duct. (**I**–**L**) Co-immunolabeling shows that GATA3 expression partially overlaps with that of NEUROD in the CVG at E9.5 to E12.5. (**M**–**P**) GATA3 is similarly expressed in a subset of ISL1+ CVG cells at E10.5–E12.5. (**Q**–**T**) Co-immunolabeling of GATA3 and TUJ1 shows that GATA3 is continuously expressed in SG from E12.5. OV, otic vesicle; CD, cochlear duct; CVG, cochlear-vestibular ganglion; SG, spiral ganglion; D, dorsal; M, medial; V, ventral; A, anterior; L, lateral. Scale bar, 50 μm.

Defective sensory organ development in the *Gata3*-null cochlea

We first analyzed the effects of *Gata3* conditional knockout on the cochlea. In wild-type mice, when the cochlea reaches its mature length at E18.5, it is approximately one and three-quarters turns and a sagittal section at the mid-modiolar level cuts through the cochlear duct at four locations (Fig. 3A). In contrast, only a miniature, short cochlear duct with no obvious turns was observed in *Gata3-null* mice and a sagittal section revealed a disorganized cochlear duct present in *Gata3-null* mutant mice (Fig. 3E). To assess the cellular defects in the cochlea of *Gata3*-null mice, we used SOX2 and MYO7A to identify supporting cells and hair cells of cochlea, respectively. Co-labeling GATA3 with SOX2 and MYO7A showed that in

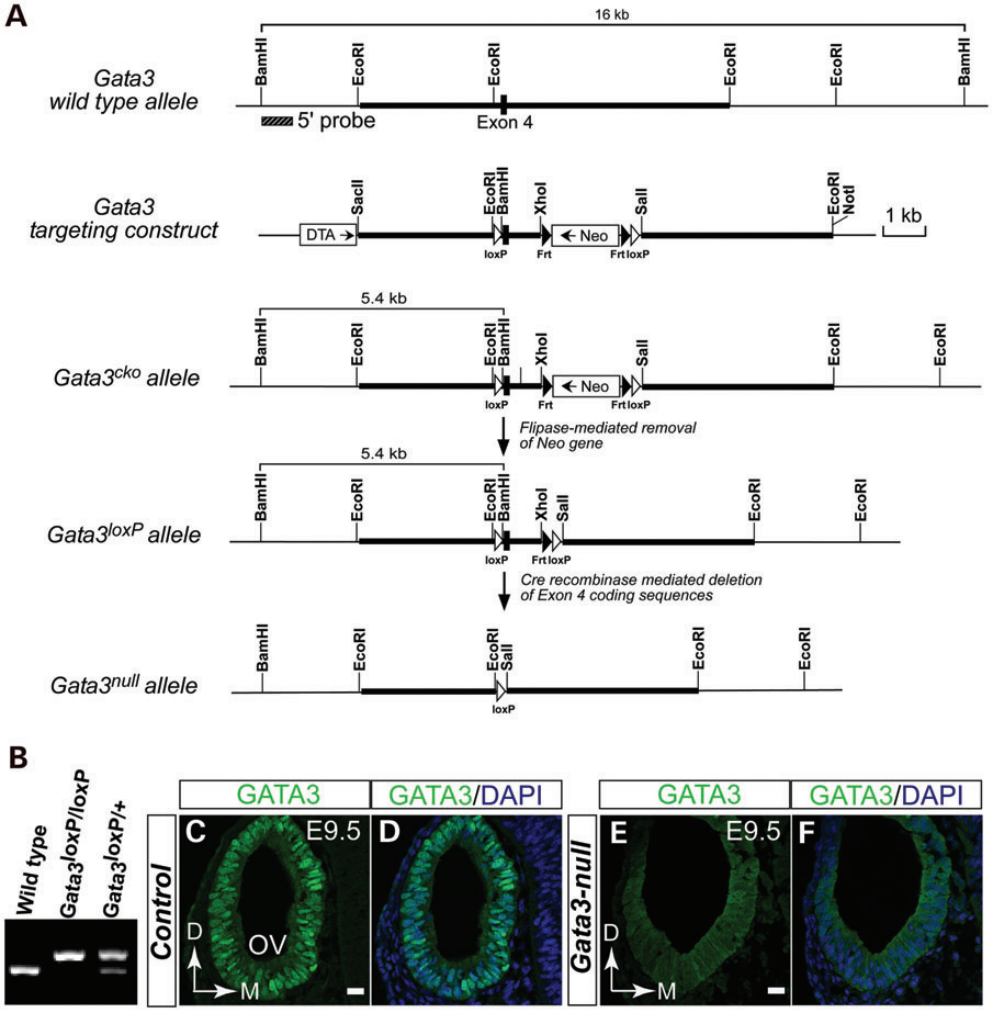

Figure 2. Inner ear-specific knockout of *Gata3* in mice. (**A**) Schematic diagram showing *Gata3* genomic structure, restriction map, and the strategy for generating *Gata3*^{loxp} mice. Black box represents Exon 4 coding sequences. Thick bars are the sequences used to generate the homologous arms in the targeting vector. The targeting vector is designed to insert loxP sites (white arrowheads) on either side of Exon 4, which encoding the first zinc-finger motif. The neomycin resistance cassette (Neo, for positive selection) is flanked by FRT sites (black arrowheads) and can be removed through crossing to FLPe-expressing mice. DTA (diphtheria toxin gene) is included for negative selection. (**B**) PCR analysis of the wild-type, heterozygous, and homozygous *Gata3* conditional knockout mice. (**C**–**F**) Immunolabeling analysis shows that *Gata3* is efficiently deleted in the otocyst of *Gata3*-null mice. In wild-type mice, GATA3 is highly expressed in the nuclei of otic epithelial cells (**C** and **D**). However, the specific nuclear expression of GATA3 is ablated in the *Gata3*-null otocyst (**E** and **F**). OV, otic vesicle. D, dorsal; M, medial. Scale bar, 20 μm.

the control cochlea at E18.5, GATA3 is highly expressed in supporting cells and weakly expressed in hair cells (Fig. 3A–D and I–K). The MYO7A-labeled hair cells are arranged in four rows in the organ of Corti along the entire length of the cochlear coil, three rows of OHCs and one row of IHCs (Fig. 3A–D, inserts). In the absence of *Gata3*, there were variable phenotypic defects in the cochlea with the patched formation of the organ of Corti-like structures, some containing supporting cells but no hair cells (Fig. 3E and F) or containing supporting cells and variable number of hair cells (Fig. 3G and H). In addition to abnormal numbers of supporting and hair cells, the orderly arrangement of hair cells was disrupted in *Gata3*-null mice (Fig. 3L–N) in contrast to the wild-type control with three rows of OHCs and one row IHCs arranged along the cochlear duct (Fig. 3I–K). Taken together, these results demonstrate that *Gata3* is important for normal development of the organ of Corti, and that disruption of *Gata3* leads to its agenesis or abnormal formation along the cochlear duct.

Developmental defects of the prosensory domain in the *Gata3*-null inner ear

The organ of Corti arises from the prosensory domain, a region in the ventral cochlear duct and is bounded by two non-sensory domains, Kölliker's organ on the neural side and the outer sulcus on the abneural side (32). The observed defects in the organ of Corti of *Gata3-null* cochlea suggest that GATA3 could regulate the specification of prosensory domain. Thus, we first investigated the morphological defects of the *Gata3-null* cochleas. While the cochlea of wide-type mice is about one turn at E13.5 (Fig. 4A), the *Gata3-null* cochlea is shorter with no obvious turn (Fig. 4B–D). In addition, the *Gata3-null* cochlea showed some degree of bifurcation at the apex region (Fig. 4B–D). We then examined whether the expression of known prosensory markers, such as SOX2 (3,33), was altered. In wild-type controls at E12.5, SOX2 is expressed in the ventral cochlea duct, largely overlapping the expression of

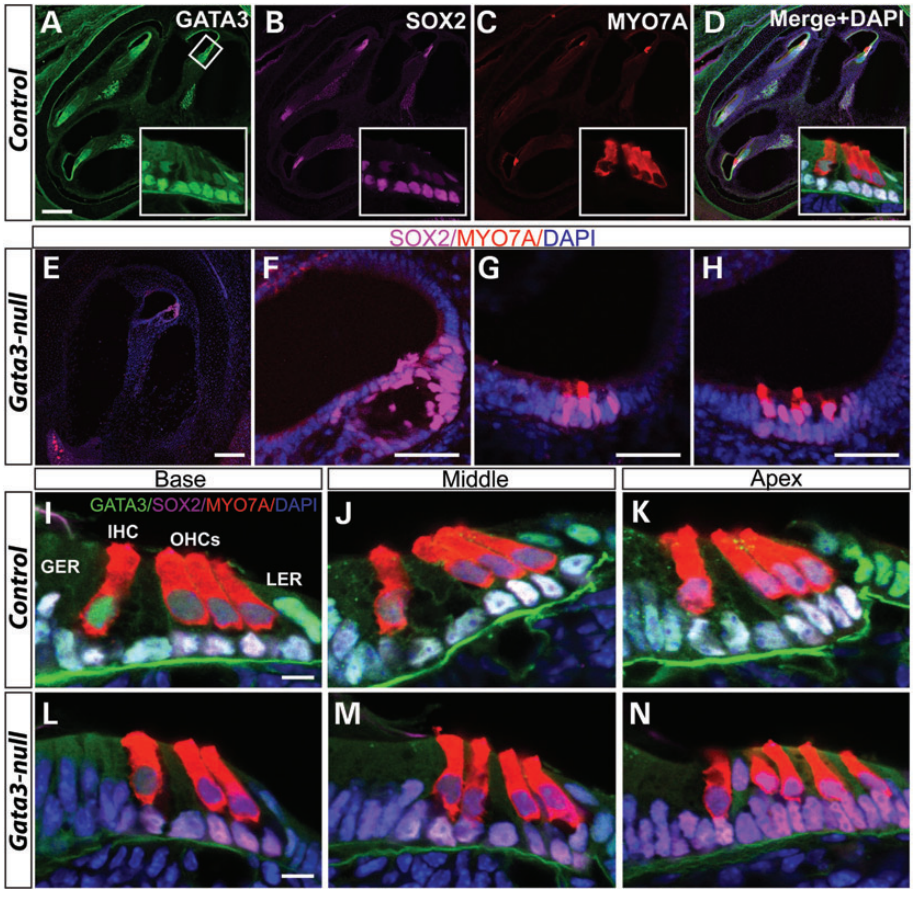

Figure 3. Abnormal hair and supporting cell patterns in the inner ear of *Gata3*-null mice. At E 18.5, co-immunolabeling shows that GATA3 is expressed in SOX2+ supporting cells and MYO7A+ hair cells. Anti-MYO7A labeling reveals the orderly arranged three rows of OHCs and one row of IHCs in wild-type mice (**A**–**D** and **I**–**K**). However, in *Gata3*-null mice, there are variable phenotypic defects in supporting and hair cells, e.g. no hair cells and with only limited supporting cells (**E** and **F**) or with limited hair cells (**G** and **H**). In addition, the patterns of hair cells are also disrupted in the inner ear of *Gata3*-null mice (**L**–**N**). For example, only two rows of OHCs are observed in the base part of cochlear duct (L). In middle part, an extra row of IHCs is detected (M). In the apex, disorganized hair cells are also observed (N). GER, greater epithelial ridge; IHC, inner hair cell (color-coded red); LER, lesser epithelial ridge; OHCs, outer hair cells (color-coded red); SCs, supporting cells (color-coded magenta). Scale bar, (A–E) 200 μm; (F–H) 50 μm; (I–N) 10 μm.

GATA3 (Supplementary Material, Fig. S2A–C). At E13.5, the expression of SOX2 becomes restricted to the newly formed prosensory domain and part of Kölliker's organ, which destines to become the inner sulcus of the cochlea (32). GATA3 is strongly expressed in the prosensory domain and the future outer sulcus at E13.5 (Fig. 4K–M). In contrast, the expression of SOX2 appeared down-regulated in the *Gata3*-null cochlea at E12.5 (Supplementary Material, Fig. S2D–F) and was greatly reduced at E13.5 (Fig. 4E–J'). Strikingly, in the *Gata3*-null cochlea, SOX2 expression domain was not all confined to the presumptive prosensory region and ectopic SOX2+ domain was seen (Fig. 4J', arrowheads, and Q–S, bracket). Furthermore, the expression of $P27^{kip1}$, another well-characterized prosensory marker (Fig. 4F and F'), was dramatically decreased in the *Gata3-null* cochlea and the mutant cochlea lacked a clearly defined prosensory region (Fig. 4I and I'). Additionally, ectopic $P27^{kip1}$ expression domains were seen in the *Gata3-null* cochlea (Fig. 4J', arrowheads). Furthermore, in wild-type mice, the expression of JAG1, *Fgf10* and *Lfng* is progressively restricted to the Kolliker's organ and that of *Bmp4* to in the outer sulcus (abneural side of the prosensory domain) at E13.5. In contrast, in *Gata3-null* mice, the expression of *Fgf10* is greatly down-regulated and the expression domains of JAG1, *Lfng* and *Bmp4* are less defined (Fig. 4T–Z). Taken together, these results demonstrate that *Gata3* plays an important role in the establishment of prosensory domain by regulating the regional expression of prosensory markers.

Elevated cell death in the cochlear duct of *Gata3*-null mice

To elucidate the molecular mechanism underlying the cochlear defect in *Gata3*-null mice, we assessed the cell death during the development of cochlea. At E12.5, CASP3+ positive cells in the cochlear duct of wild-type mice were hardly detected (Fig. 5A). In contrast, numerous CASP3+ positive cells were detected in the cochlear duct of *Gata3*-null mice ($P < 0.0001$, Fisher's exact test) (Fig. 5B and C). Similar increases in apoptosis were seen in the *Gata3*-null cochlea at E13.5 (Fig. 5D–I) as well as at E14.5 (Fig. 5J–O). Thus, the loss of *Gata3* triggers massive cell death during the early development of the cochlear duct. Interestingly, the observed cell death occurs beyond the prosensory region in the *Gata3-null* inner ear at E13.5

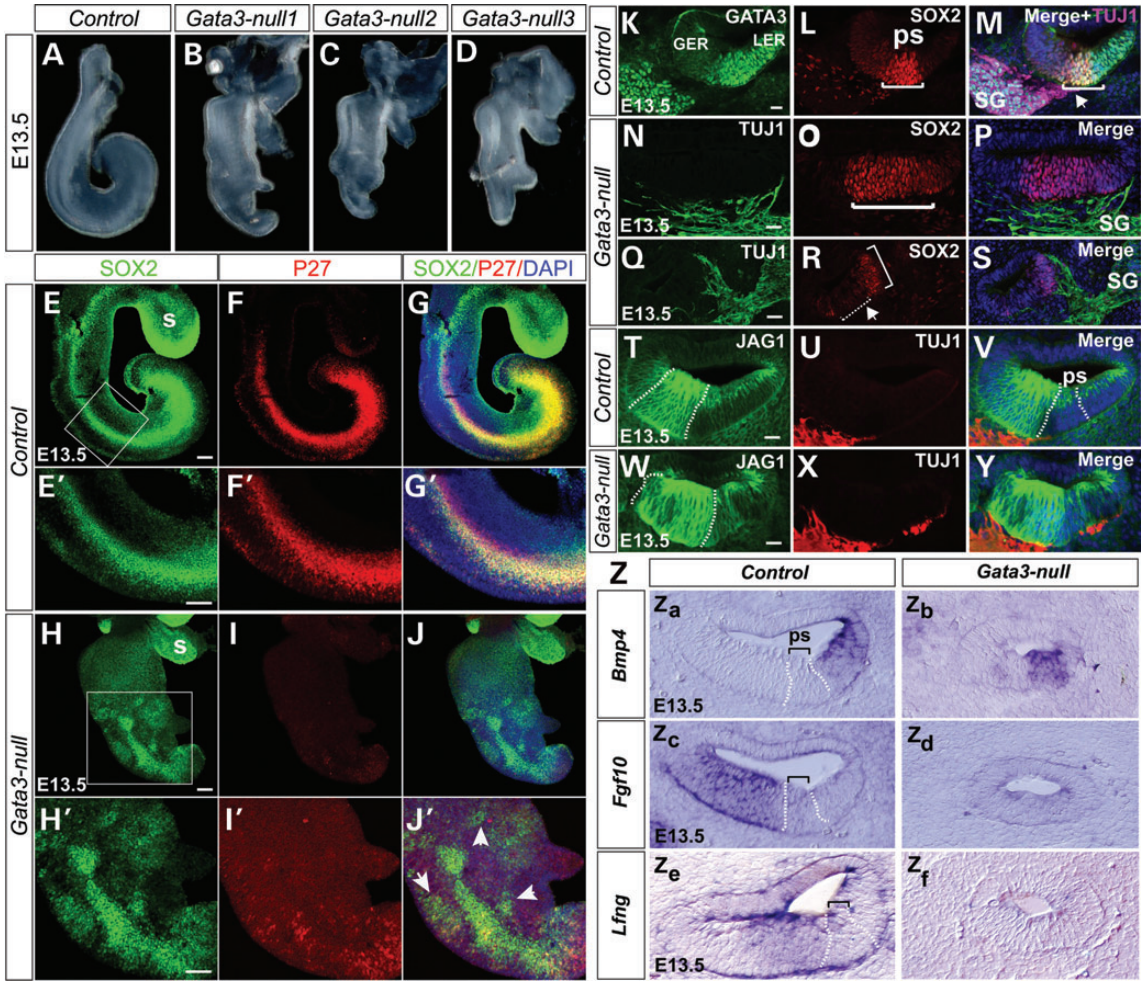

Figure 4. *Gata3* is required for the establishment of the prosensory domain and the axon targeting process of SGNs. (**A**–**D**) Compared with the cochlea of wide-type mice (A), the cochleas of *Gata3-null* mice are shorter with no obvious turn and show some degree of bifurcation at the apex region (B–D). Three representative cochleas of *Gata3-null* mice are shown. (**E**–**J**′) Failure of prosensory domain establishment in *Gata-3 null* mice at E13.5. Whole mount immunohistochemistry reveals the dramatically decreased expression of SOX and $P27^{kip1}$ as well as ectopic expression (arrowheads in J') in the *Gata-3 null* cochlea. (**E**′–**J**′) High magnification of the boxed region in (E)–(J). (**K**–**S**) Anti-SOX2 and anti-GATA3 labeling shows the broader (**N**–**P**) or ectopic prosensory regions in *Gata3*-null mice. In addition, compared with the projections of SG specifically to the prosensory domain in wild-type mice (arrow head in **M**), the projections of SG are not specific in *Gata3*-null mice (N–P). (**T**–**Y**) Immunolabeling shows the altered expression pattern of JAG1 in the *Gata3-null* cochlea (**Z**) *In situ* hybridization analysis of *Bmp4* and *Fgf10* at E13.5, In *Gata3-null* mice, the expression of *these genes* is less defined. In addition, the expression of *Fgf10* is down-regulated in *Gata3-null* mice. GER, greater epithelial ridge; LER, lesser epithelial ridge; ps, prosensory domain; SG, spiral ganglion neurons. s, saccule, Scale bars (E–J′) 100 μm (K–Y) 25 μm.

(Fig. 5G–I). Though GATA3 is mainly expressed in the prosensory domain and the future outer sulcus in wide-type mice at E13.5 (Fig. 4K–M), it is expressed in a broad region in the otic vesicle (Fig. 1A) and in the cochlear duct (Supplementary Material, Fig. S3) at early developmental stages, suggesting that the early GATA3 expression might be required for cell survival in the non-sensory region.

Loss of SGNs in *Gata3*-null inner ears

The hair cells receive and transform sound vibrations in the cochlea into electrical signals that are then relayed by SGNs to the auditory brainstem and to the auditory cortex. Abnormalities in hair cells or SGNs cause human sensorineural hearing loss, the most common sensory deficit in developed countries (34). Interestingly, sensorineural deafness is one of the typical symptoms of HDR syndrome caused by *GATA3* haplo-insufficiency. Our above data have indicated that *Gata3* is required for the normal development of the organ of Corti. However, whether *Gata3* has a role in the development of SGNs is not known.

SGNs are derived from neuroblasts that delaminate from the ventral region of the otocyst at E9.5. Around E10.5, these neuroblasts coalesce adjacent to the developing inner ear and form the CVG (28). As development continues, the CVG neurons separate into vestibular and cochlear ganglia, and complete their migration by E14.5. The expression of GATA3 in developing CVG neurons prompts us to investigate the role of *Gata3* in the development of SGNs. In the control cochlear section at E18.5, TUJ1 immunolabeling revealed numerous SGNs, SGN fibers contacting with the base of hair cells, and bundled SGN axons forming

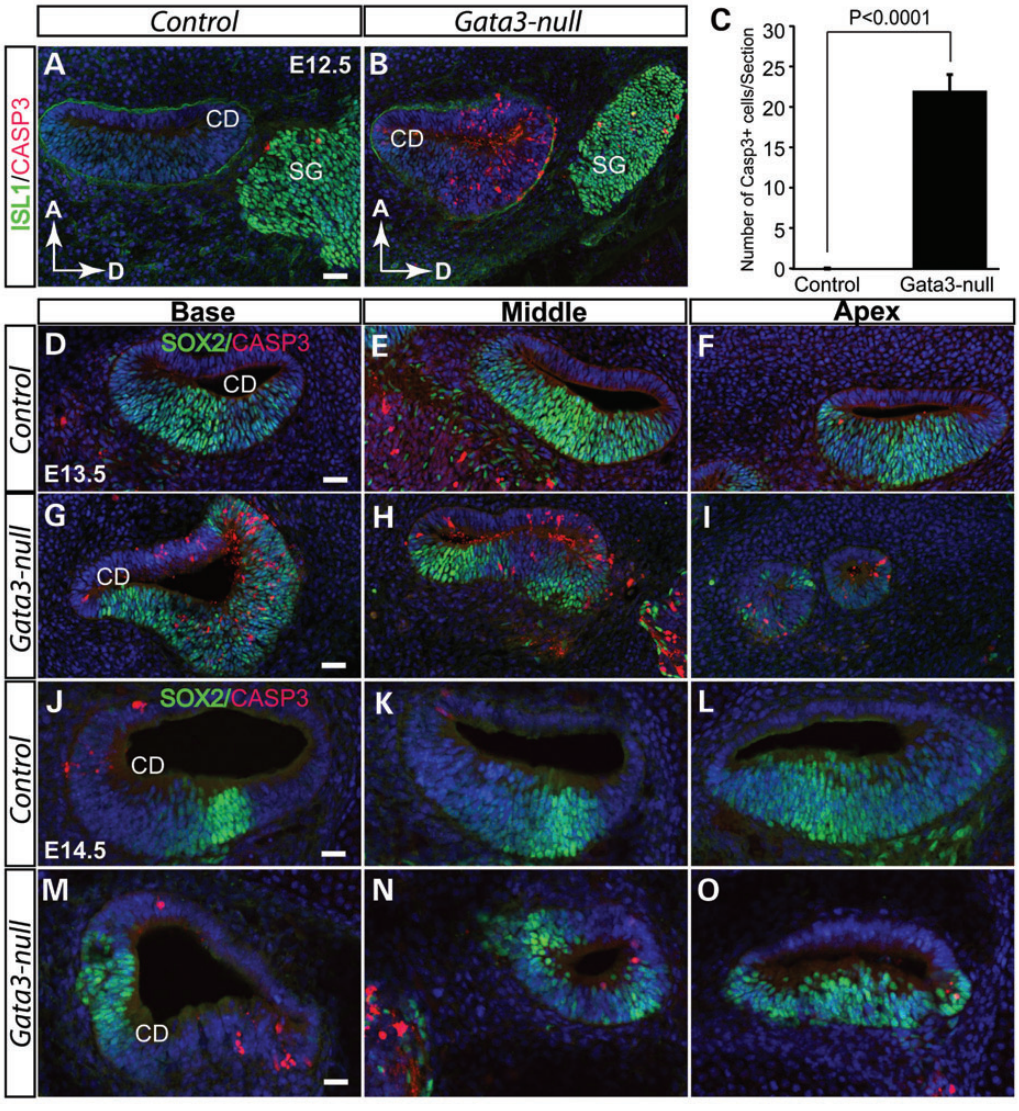

Figure 5. Elevated cell death in the cochlear duct of *Gata3*-null mice. (**A** and **B**) At E12.5, no CASP3+ apoptotic cells are detected in wild-type mice (A). However, cell death is greatly increased in the cochlear duct of *Gata3*-null mice (B). (**C**) Quantification of apoptotic cells ($CASP3^{+}$/section) in the cochlear duct ($P < 0.0001$, Fisher's exact test, $n = 3$ for *Gata3*-nulls and $n = 3$ for controls). (**D**–**I**) Cell apoptosis analysis reveals dramatically elevated cell death in the cochlear duct of *Gata3*-null mice at E13.5. By E14.5, the structure of the cochlear duct is disrupted in *Gata3*-null mice due to cell death (**J**–**O**). Compared with wild-type mice, the cochlear duct is much smaller in *Gata3*-null mice. Data are shown as the mean ± SEM. CD, cochlear duct; SG; spiral ganglion neurons; D, dorsal; A, anterior. Scale bar, 50 μm.

the auditory portion of the eighth cranial nerve (Fig. 6A–H). In *Gata3*-null cochlea, very few TUJ1+ cells were observed, indicating the loss of nearly all SGNs (Fig. 6I–P). Dil-labeling further confirmed the loss of the spiral ganglion in *Gata3*-null mice at E18.5 (Fig. 9J). Therefore, *Gata3* plays an essential role in the development of SGNs and conditional knockout of *Gata3* leads to the depletion of the spiral ganglion.

Apoptosis of the SGNs during early development

To test if the loss of SGNs was a result of reduced cell proliferating in *Gata3*-null mice, we assessed the cell proliferation by immunolabeling with anti-pH3, a marker for proliferating cells. Analysis of cell proliferating at early developmental stage revealed that there is no significant change in the number of pH3+ cells in the CVG at E11.5 ($P = 0.48$, two-tailed *t*-test) (Fig. 8A–G), indicating that the cell proliferation rate in the cochlear duct (sensory epithelium) and CVG was not affected in *Gata3*-null mice.

Since GATA3 is expressed throughout the development of SGNs, it could be essential for the initial generation of SGNs or it is indispensable for the survival of SGNs. To distinguish these possibilities, we first analyzed neuronal differentiation using NEUROD and ISL1 as the markers for CVG cell specification and differentiation, respectively. Compared with the controls, anti-NEUROD immunolabeling revealed a normal delamination and initial formation of CVG neurons in *Gata3*-null mutants at E9.5 to E12.5 (Fig. 7A–H). Similarly, the onset of ISL1 expression in the CVG neurons is comparable between the control and *Gata3*-null mice (Fig. 7I–P). Taken together, these results indicate that the initial generation of CVG neurons is not affected by *Gata3* conditional knockout.

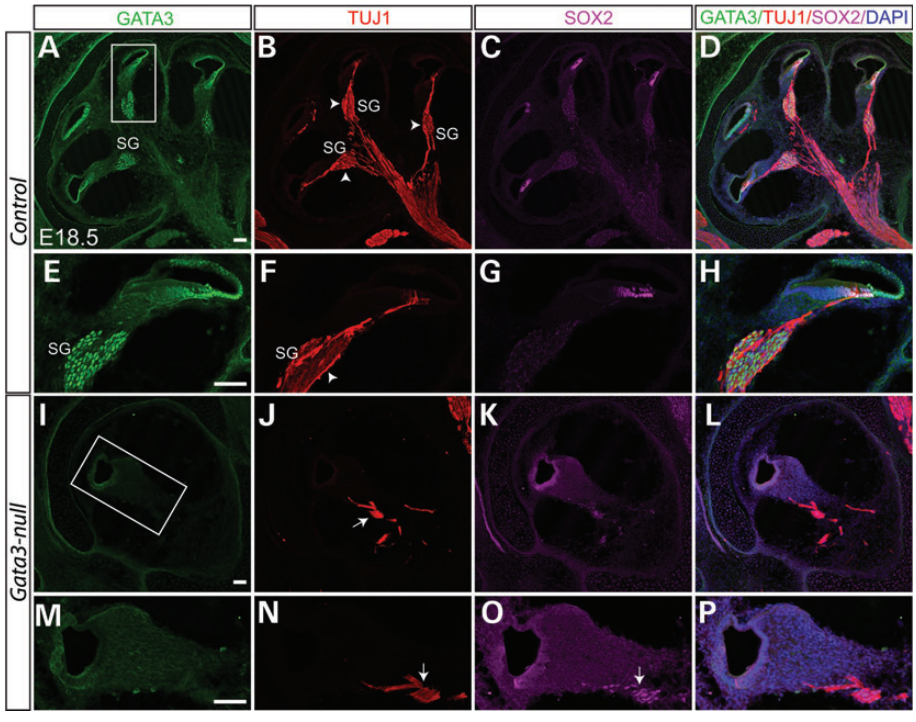

Figure 6. Depletion of SGNs in *Gata3*-null mice. (**A**–**D**) Triple-immunolabeling shows that GATA3 is highly expressed in the SOX2+ supporting cells and the TUJ1+ SGNs. The peripheral processes of SGNs make synaptic contact with the hair cells while the SGN axons are bundled together to form the auditory portion of eighth cranial nerve (B–D). Contrasting to the numerous SGNs in wild-type mice (arrowhead in B and **F**), the SGNs are nearly depleted (**I**–**P**) and very limited fibers remained (arrow in J and N) in *Gata3*-null mice. (E–H and M–P) High magnification of boxed regions in (A) and (I). Scale bar, 100 μm.

We then asked if the loss of SGNs in *Gata3*-null mice resulted from apoptosis. We co-labeled cochlear sections at E12.5 with anti-CASP3 and quantified the proportion of apoptotic neurons in the CVG. The number of apoptotic SGNs was significantly increased in *Gata3*-null CVG compared with the control at E12.5 to E14.5 (Fig. 8H–M). Quantification of the CVG neurons at E12.5 showed that there were ∼40% less ISL1+ CVG neurons in *Gata3*-null than in the control at E12.5 ($P < 0.05$, Fig. 8N) and that the ratio of apoptotic neurons ($CASP3^{+}$/ $ISL1^{+}$) was increased by 1.7-fold in *Gata3*-null mice compared with wild-type mice at E12.5 ($P < 0.05$, Fig. 8O). Collectively, these results suggest that SGNs in the CVG might undergo extensive apoptosis and demonstrate that *Gata3* is an essential survival factor for SGNs.

Auditory fibers and projection defects in the inner ear of *Gata3*-null mice

Auditory neurons are bipolar neurons that consist of the peripheral processes (the most distal portion) and centrally projecting axons. Their projections are also known as the peripheral axons (dendrites) and the central axons. To further investigate if the loss of SGNs affected the extent and global pattern of SGNs in *Gata3*-null mice, we labeled the fibers of SGNs by DiI-labeling and TUJ1 immunohistochemistry. In the vestibular system, the neural fibers to the posterior and horizontal cristae were absent in *Gata3*-null mice while those to the utricle and anterior cristae appeared normal (Fig. 9C and D). Moreover, the superior vestibular ganglia are comparable in the control and *Gata3*-null, but the inferior vestibular ganglion was not detected in *Gata3*-null mice (Fig. 9E and F).

In the cochlea, SGNs position their cell bodies in the modiolus, extend their dendrites to make synaptic contacts with hair cells and SGN axons bundle together to form the auditory portion of the eighth cranial nerve. Compared with the readily detected SGNs and their projections to the hair cells in the base, middle and apex of the control cochlea (Fig. 9G–I), only limited spiral ganglion-like structure was observed in *Gata3*-null mice, but no SGN bodies and SGN fibers to the hair cells were observed (Fig. 9J). These results further confirm the loss of SGNs in *Gata3*-null mice.

Global gene expression profiling in the inner ear of *Gata3-null* mice

Gata3 is a transcription factor that regulates the expression of target genes. To determine the change in transcriptome in the absence of *Gata3*, we performed RNA-Seq analysis of wild-type and *Gata3*-null inner ears. Analysis of RNA-Seq results (sequencing reads mapped to the exon 4 of *Gata*3) indicated that the exon 4 of *Gata*3 was efficiently deleted in the inner ear of *Gata*3-null mice (Supplementary Material, Figs S3 and S4). Among the 876 genes identified with significant expression change (corrected $P < 0.05$), 727 genes were significantly down-regulated and 149 genes were significantly up-regulated in the *Gata3-null* inner ear (Supplementary Material, Fig. S5A). Using real-time

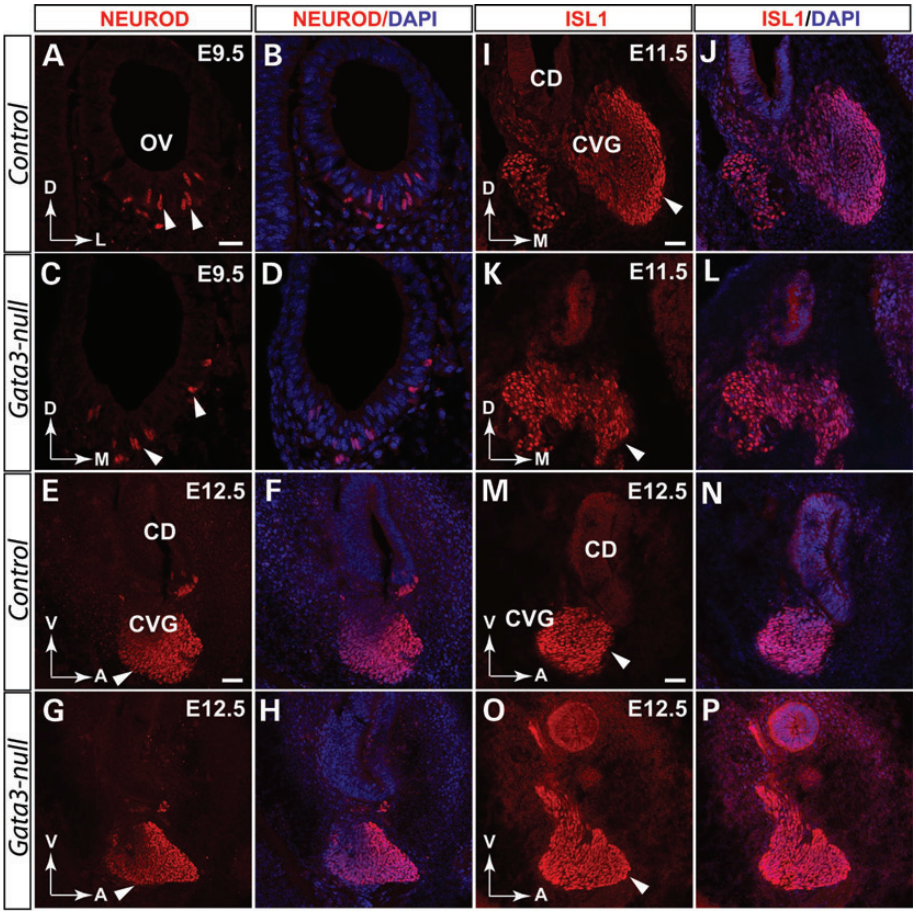

Figure 7. Loss of *Gata3* does not affect the initial generation of CVGs. Double-immunolabeling shows that GATA3 is expressed in the developing CVG. (**A**–**D**) Deletion of *Gata3* does not significantly affect the generation of CVG neurons as comparable NEUROD+ cells (arrowheads in **C**) are generated in *Gata3*-null mice. Similar results are obtained when a different developmental stage (E12.5) were analyzed (**E**–**H**). (**I**–**L**) At E11.5, the deletion of *Gata3* has no detectable effect on the generation of ISL1+ CVGs. (**M**–**P**) Further analysis revealed that ISL1+ CVG neurons are not significantly changed at E12.5. OV, otic vesicle; CVG, cochleovestibular ganglion. CD, cochlear duct. D, dorsal; M, medial; V, ventral; A, anterior; L, lateral. Scale bar (A–D) 25 μm. (E–P) 50 μm.

quantitative PCR, we validated the RNA-Seq results by testing five selected genes (*Apod*, *Cdk*1, *Phgdh*, *Rpsa* and *Rps*17) (Supplementary Material, Fig. S5B). *Apod* encodes a component of high-density lipoprotein. *Cdk*1encodes a serine/threonine kinase (CDK1), a key regulator of cell cycle. *Phgdh* encodes D-3-phosphoglycerate dehydrogenase, an enzyme that catalyzes the transition of 3-phosphoglycerate into 3-phosphohydroxypyruvate. *Rpsa* and *Rps*17 encode 40S ribosomal protein SA and 40S ribosomal protein S17. Gene Ontology (GO) analysis revealed multiple biological processes were disturbed in the *Gata3-null* mice (Supplementary Material, Fig. S5A). In particular, the translation and ribosome biogenesis related genes were significantly enriched in the down-regulated genes.

Of the genes expressed in the cochlea during the establishment of the prosensory domain, the expression of *Sox2*, *Fgf10* and *Id2* (a known BMP target gene) is down-regulated, while the expression of *Jag1* and *Bmp*4 is slightly up-regulated in the *Gata3-null* inner ears (Supplementary Material, Fig. S5D), consistent with the *in situ* hybridization and immunolabeling results (Fig. 4) and further supporting the essential role of *Gata3* in regulating the regional expression of prosensory markers during prosensory domain development.

DISCUSSION

HDR syndrome is an autosomal dominant disease caused by *GATA3* haploinsufficiency. Haploinsufficiency is attributed to deletions (including deletion of one allele and in-frame deletion) (11), or point mutations (including missense mutation and non-sense mutation) of the *Gata3* gene (35,36). The hypoparathyroidism leads to a lower level of calcium in blood, lifelong fatigue and depression. The sensorineural deafness is congenital and the kidney dysplasia causes nephrosis and progressive renal failure. Though recent studies revealed the important role of GATA3 in the development of the kidney and the parathyroid (13,14), and several studies have explored the function of *Gata3* in mouse inner ear development (16,24,27), the exact role of *Gata3* in the development and function of inner ear remains elusive as the conventional *Gata3* knockout mice die at early developmental stage (around E13.5). In this study, we have utilized conditional knockout strategy to inactivate *Gata3* specifically in the developing inner ear and have shown that the loss of *Gata3* causes severe inner ear defects including the defective formation of the cochlear prosensory domain and a significant loss of SGNs. Thus, our

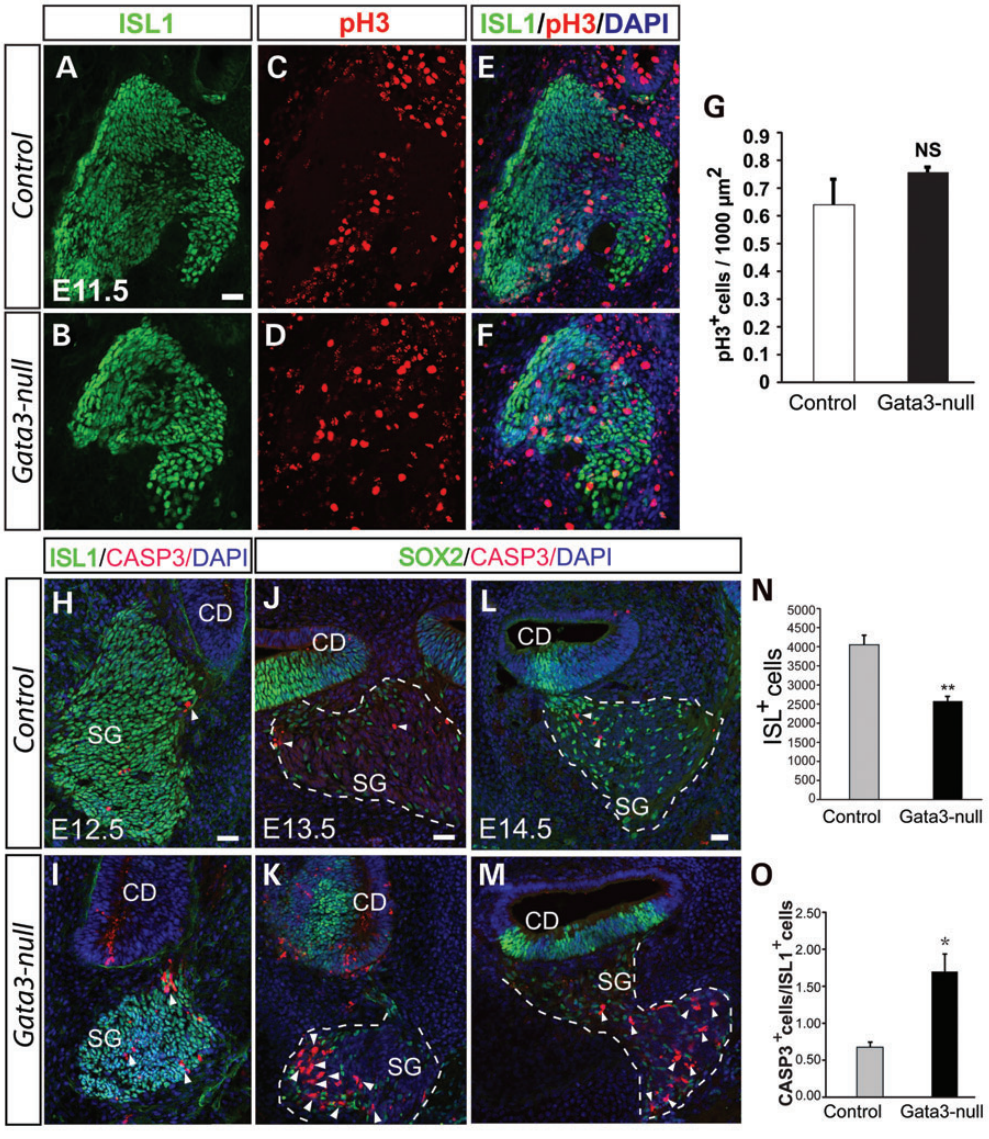

Figure 8. *Gata3* is required for the survival of SGNs. (**A**–**J**) Quantification of cell proliferation in the CVG shows no significant change of cell proliferating in *Gata3*-null mice ($n = 3$ for wild-types and $n = 4$ for *Gata3*-nulls). Data are shown as the mean ± SEM. NS, not significant. (**H**–**I**) The number of CASP3+ apoptotic cells is greatly increased in the spiral ganglion of *Gata3*-null mice. (**J**–**M**) Further analysis of cell death at E13.5 and E14.5 shows dramatically elevated cell death of SGNs in *Gata3*-null mice. (**N**) The number of ISL1+ CVG neurons is significantly decreased in *Gata3*-null mice at E12.5 ($^*P < 0.001$, two-tailed Student's test, $n = 4$ for mutants and $n = 5$ for controls). (**O**) Quantification of cell apoptosis rate ($CASP3^+/ISL1^+$) in spiral ganglion at E12.5 reveals greatly increased cell death in *Gata3*-null mice ($^*P < 0.05$, two-tailed Student's test, $n = 3$). CD, cochlear duct; SG, spiral ganglion neurons. Scale bars, 50 μm.

results present direct evidences to support the role of *Gata3* in HDR diseases.

Role of *Gata3* in the developing sensory region

Gata3 is expressed early in the otocyst at E9.5 and is continuously expressed in the cochlea during the formation of the sensory organ. At E12.5, GATA3 is expressed in the cochlear duct and its expression is detected in the prosensory domain and the future outer sulcus at E13.5 (Fig. 4K–M). Co-labeling study in the prosensory domain indicated that GATA3 is co-localized with SOX2, a well-characterized marker for the prosensory domain. Consistently, conditional knockout of *Gata3* in mice lead to a severe developmental defect of the mouse inner ear. It is possible that *Gata3* may regulate the morphogenesis of the inner ear as the gross structure of the inner ear is severely affected in *Gata3*-null mice (Fig. 9). Additionally, the structure of the cochlear duct is severely disrupted in *Gata3*-null mice and an elevated apoptosis level is observed in the developing cochlea. Strikingly, the loss of *Gata3* also results in the absence or ectopic formation of the organ of Corti, or in the generation of the organ of Corti-like structure with hair cells missing or disorganized. These results suggest the essential role of *Gata3* in the development of the cochlear sensory organ. Indeed, we have shown that the refinement of SOX2 and $P27k^{ip1}$ expression in the prosensory domain is disrupted in *Gata3*-null mice

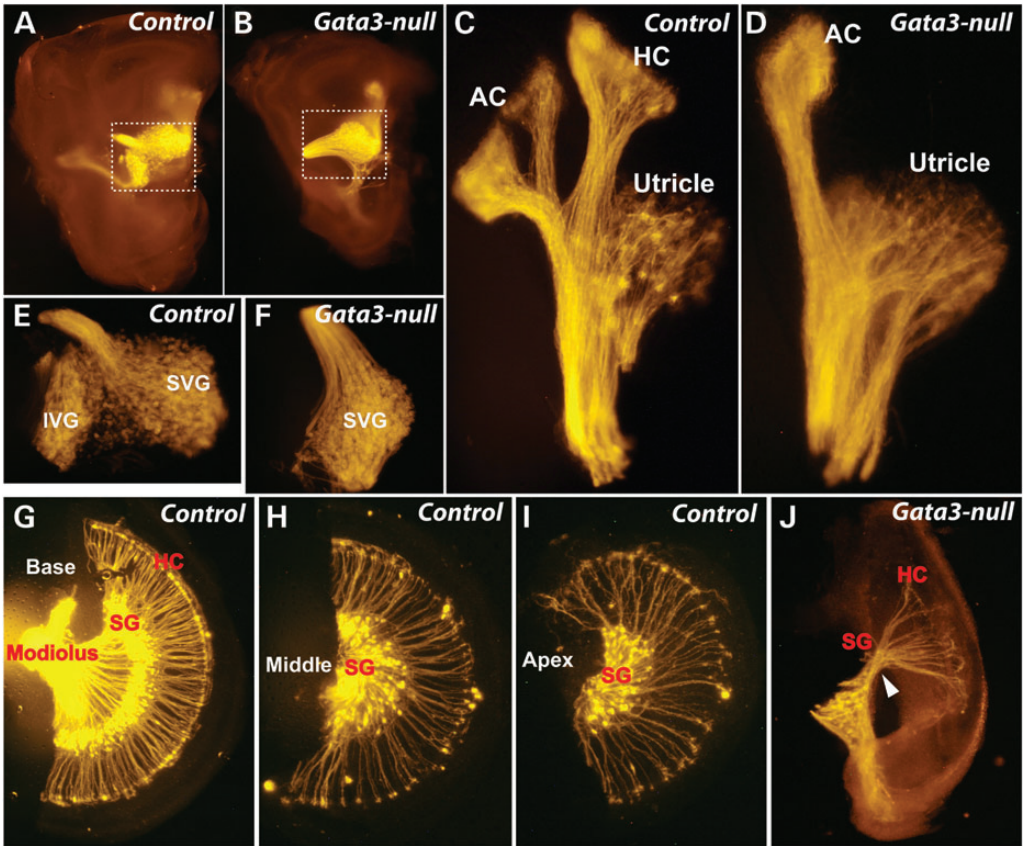

Figure 9. Morphological and projection defects of the vestibular and spiral ganglia in *Gata3*-null mice. (**A** and **B**) *Gata3*-null mouse has a smaller inner ear. (**C** and **D**) Defects of vestibular system in *Gata3*-null mice. The utricle and anterior cristae seem normal whereas the horizontal crista is absent in *Gata3*-null mice. (**E** and **F**) The superior vestibular ganglion (SVG) is normal while the inferior vestibular ganglion (IVG) is missing in *Gata3*-null mice. (**G**–**I**) The cochlea of normal mice is composed of base, middle and apex parts. The peripheral processes of SGNs form radial bundles that project through otic mesenchyme to make synaptic contact with hair cells, and the axons are bundled together to send fibers into the central nervous system. (**J**) The size of *Gata3*-null cochlea is about one-third of the controls. Most SGNs and hair cells are depleted in *Gata3*-null mice. In addition, the projection of SGNs is disrupted. AC, anterior cristae; HC, horizontal cristae; IVG, inferior vestibular ganglion; SVG, superior vestibular ganglion; HC, hair cells; SG, spiral ganglia.

(Fig. 4), demonstrating GATA3's direct involvement in the specification of the prosensory domain in the cochlea. We also found the expression of SOX2 and $P27^{kip1}$ is severely reduced in the *Gata3-null* cochlea at E13.5 (Fig. 4). Considering the importance of SOX2 and $P27^{kip1}$ in prosensory domain development, our results imply that the defective prosensory domain development in the *Gata3-null* cochlea is likely due to the disruption of these proteins. Moreover, the regional expression pattern of JAG1, *Bmp4* and *Fgf10* was also disturbed in the cochlea of *Gata3-null* mice (Fig. 4). Taken together, these results indicate that *Gata3* plays pivotal roles in prosensory domain development through regulating and restricting the expression pattern of the well-characterized prosensory markers.

Previously, Ohyama *et al.* (32) found that *Bmp4* is expressed in the future outer sulcus at E13.5 and BMP signaling is necessary for patterning the sensory and non-sensory regions of the developing mouse cochlea. The expression of *Gata3* in the outer sulcus suggests that GATA3 could regulate the patterning of the sensory region by regulating BMP4 expression in the inner ear. A published study by Ralston *et al*. (37) has shown that *Gata3* induces the expression of *Bmp4* and *Notch1* in trophoblast, supporting the notion that GATA3 may regulate the expression of BMP4 during the sensory domain development in the inner ear. However, our *in situ* hybridization, real-time quantitative PCR and RNA-Seq data revealed that the expression level of *Bmp4* is not significantly changed in *Gata3-null* mice (Fig. 4Zb, Supplementary Material, Fig. S5C and D). Interestingly, the expression of *Id2*, a known BMP target gene, is downregulated in *Gata3-null* mice (Supplementary Material, Fig. S5D), suggesting that GATA3 could control the patterning the sensory and non-sensory regions of the developing mouse cochlea by regulating BMP pathway genes. In the absence of *Gata3*, the specification of the prosensory domain is disrupted, resulting in the absent or abnormal formation of the prosensory domain, or an ectopic formation of the prosensory domain in the outer sulcus region. Considering the expression of *Gata3* in the prosensory domain and the outer sulcus region, the mechanisms of GATA3 function are likely unique to each region, depending on the combinatory effects of region-specific regulators yet to be identified.

Furthermore, our *in situ* hybridization and RNA-Seq results indicate that the expression of *Fgf10* is significantly downregulated in *Gata3-null* mice at E13.5 (Fig. 4Z, Supplementary Material, Fig. S5D), while the expression of FGF receptors (*Fgfr1* and *Fgfr2*) was not significantly changed according to RT–qPCR results (Supplementary Material, Fig. S5C).

Intriguingly, recent studies have revealed that *Gata3* directly regulates the expression of *Fgf10* in the mouse inner ear through binding to the promoter region of *Fgf*10 (24,38). Collectively, these results indicate that *Fgf*10 is likely a direct target of *Gata*3 in the developing inner ear. Given the importance of FGF signaling in the development of the mouse inner ear (39–46), the morphological defects observed in *Gata3-null* mice may be caused by the dysregulation of FGF signaling.

Gata3 is essential for SGN survival

One of the key findings in this study is the loss of SGNs in *Gata3*-null mice. SGNs are a specific cell population that relays sound signals to the central nervous system. Two apparent subtypes of SGNs are defined in mammals (47). Type I SGNs account for 95%, whereas type II SGNs make up the remainder. From the aspect of morphology, type I SGCs are larger and are responsible for the sensory innervation of the IHCs of the organ of Corti (47). Though GATA3 is expressed in CVGs at the early stage of inner ear development (from E9.5 to E12.5), the initial generation of CVGs is not affected by *Gata3* conditional knockout as a normal number of CVG neurons positive for NEUROD and ISL1 are generated in *Gata3*-null mice (Fig. 7). Our expression analysis of GATA3 in SGNs shows that GATA3 is highly expressed in SGNs from E13.5. More importantly, SGNs are mostly depleted in *Gata3*-null mice at E18.5. These data further support GATA3 as an important pro-survival factor for SGNs. SGNs extend their fibers and make synaptic contact with hair cells during inner ear development. The defect in this process observed in *Gata3*-null mice could result in the lack of neurotropic factor feedback from the hair cells, which may indirectly trigger the death of SGNs. However, both our data and previous studies argue for a cell-autonomous death of SGNs in *Gata3*-null mice. First, the onset of SGN death in *Gata3*-null mice starts at E12.5 (Fig. 7), an early developmental stage before hair cells are differentiated and before most of SGNs extend their fibers to hair cells. Second, hair cells are not required for the survival of SGNs in the adult cochlea (48), further supporting that the observed death of SGNs in *Gata3*-null mice is not due to the defects in hair cells or axon targeting. The number of apoptotic cells is greatly increased in the *Gata3*-null cochlear duct at E12.5 to E14.5, arguing again for a pro-survival role of *Gata3*. Previous study has shown that *Gata3* promotes the survival of embryonic and adult sympathetic neurons through regulating anti-apoptotic (*Bcl-2*, *Bcl-xl*) and pro-apoptotic (*Bik*, *Bok*, *Bmf*) genes (49). However, our real-time quantitative PCR and RNA-Seq data revealed no overt change in the expression of anti-apoptotic (*Bcl-2*, *Bcl-xl, Jun*) and pro-apoptotic (*Bik*, *Bok*, *Bmf, Bad*) genes in the *Gata3-null* inner ear (Supplementary Material, Fig. S6), suggesting a different role of *Gata*3 in inner ear and sympathetic neurons. Since the failure of neurotrophin receptor expression could cause the death of SGNs (8), we further examined the expression of neurotrophins (e.g. BDNF and NGF) and their receptors (*Trk A, Trk B, Trk C* and *Ngfr*) by RNA-Seq, and found that no significant down-regulation in their expression in the *Gata3-null* mice inner ear (Supplementary Material, Fig. S6), suggesting that the death of SGNs observed in *Gata3-null* mice is unlikely due to failure of expression neurotrophins and their receptors. Interestingly, further GO analysis revealed that translation and ribosome biogenesis-related genes were significantly enriched in the down-regulated genes in the *Gata3-null* inner ear (Supplementary Material, Fig. S5). As inhibition of ribosome biogenesis and decrease in protein synthesis could cause apoptosis (50), it is possible that the dysregulation of these genes is associated with the cell death in the *Gata3-null* inner ear.

Gata3 is required for proper axon projection of SGNs

SGNs arise from neuroblasts that delaminate from the otocyst at early developmental stage (E9.5). By E12.5, SGNs send projections toward the cochlear duct (peripheral projection) and hindbrain (axon guidance) (Supplementary Material, Fig. S2A–C). By E13.5, peripheral projections from SGNs specifically targeted the prosensory domain, the presumptive organ of Corti (Fig. 4K–M). We found that the peripheral projections in *Gata3*-null mice are severely affected (Fig. 4N–P). The SGN fibers in *Gata3*-null mice fail to make precise connections to the prosensory domain. Interestingly, a previous study also found that *Gata3* alters pathway selection of the olivecochlear neurons (16). These consistent results suggest that *Gata3* is involved in the pathfinding of SGNs. Nevertheless, how *Gata3* control the projection/pathfinding is not clear, further works are needed to elucidate the underlying mechanisms. In summary, we demonstrated that *Gata3* is an essential gene for the development of the mouse inner ear. Our results provide critical complementary data along with the genetic findings from human HDR syndrome to demonstrate the role of *Gata3* in the development and disease of the inner ear.

MATERIALS AND METHODS

Generation of *Gata3* conditional knockout allele

To generate the *Gata3* conditional knockout ($Gata3^{cko}$) allele, we flanked the exon 4 of *Gata3* with loxP sequences (Fig. 2A). Briefly, a 3.9 kb SacII-XhoI fragment containing the floxed Exon 4 as the 5′ homologous arm and a 4.4 kb SalI-EcoRI fragment as the 3′ homologous arm were subcloned into the SacII/XhoI and SalI/EcoRI sites of the targeting vector containing a FRT-flanked neomycin resistance gene cassette (Neo, for positive selection) and the diphtheria toxin gene (DTA, for negative selection). The $Gata3^{cko}$ construct was electroporated into G4 embryonic stem (ES) cells (51) and targeted ES cells were identified by Southern blotting. The $Gata3^{cko}$ chimeras were created by injecting the targeted ES cells into the blastocysts of C57BL/6J mice (The Jackson Laboratory, Stock Number: 000058) and were bred to C57BL/6J mice to generate $Gata3^{cko}$ mice. We then crossed $Gata3^{cko}$ mice with ROSA26-FLPe mice (The Jackson Laboratory, Stock Number: 003946) to remove the FRT-flanked Neo gene to generate $Gata3^{loxP/+}$ mice. The $Pax2^{cre}$; $Gata3^{loxP/loxP}$ (*Gata3* conditional knockout, hereafter called *Gata3*-null) mice with *Gata3* specifically deleted in the inner ear were generated through breeding of $Gata3^{loxP/+}$ with $Pax2^{cre}$ mice (31). The $Gata3^{loxP}$ allele was confirmed by the Southern blot. PCR methods were used to genotype mice from subsequent breeding of $Gata3^{loxP}$ mice (Fig. 2B). The PCR primers used to identify wild-type, heterozygous ($Gata3^{loxP/+}$), and homozygous ($Gata3^{loxP/loxP}$) alleles were 5′-TATGTCAGGGCACTAAGGGTTGTT-3′ and

5′TTAGGGAAGGAAAGCGTGTGAAA-3′. Embryos were identified as E0.5 at noon on the day at which vaginal plugs were observed. All animal procedures used in this study were approved by The University Committee of Animal Resources (UCAR) at University of Rochester.

Dil-labeling

The Dil-labeling was performed as previously described (8). In brief, P0 mice were deeply anesthetized, transcardially perfused with 4% PFA. The heads were then cut sagittally at the midline, lipophilic dye DiI (Molecular Probes) was applied to the alar plate rostral to the statoacoustic (octaval) nerve root in P0 G*ata3-null* mice and their wild-type littermates ($n = 3$ for each genotype). After 3 weeks incubation in 4% PFA at 37°C, the inner ears were dissected and examined with a fluorescence microscope and images were captured by a Zeiss 510 confocal microscope.

Immunohistochemistry

Immunohistochemistry was performed as previously described (52). In brief, embryos were fixed in 4% PFA in PBS for 1 h to overnight according to their developmental stages, and cryoprotected in 30% sucrose in PBS before rapid freezing in OCT compound (TissueTek). The cryosections were cut at a thickness of 20 μm. For antigen retrieval, cryosections (20 μm) were heated at 96°C for 10 min in 10 mM citrate buffer (pH 6.0, with 0.05% Tween-20) and then cooled down gradually to room temperature. The sections were permeabilized and blocked in PBS plus 0.3% Triton-X100, 5% horse serum, incubated with primary antibody overnight at 4°C, washed in PBS three times, and incubated with fluorescently labeled secondary antibody for 1 h at room temperature. The primary antibodies used were mouse anti-GATA3 (BD Pharmingen, 1:200), goat anti-SOX2 (Santa Cruz, 1:500), rabbit anti-MYO7A (Proteus Biosciences, 1:1000), rabbit anti-TUJ1 (Covance, 1:1000), goat anti-NEUROD (Santa Cruz, 1:500), mouse-anti-ISL1 (DSHB, 1:500), rabbit anti-ISL1 (Abcam, 1:200), rabbit anti-CASP3 (RD systems, 1:250) and rabbit anti-phospho-Histone H3 (pH3) (Santa Cruz, 1:400). Alexa Fluor-conjugated donkey anti-mouse, rabbit or anti-goat (Invitrogen, 1:500) was used as secondary antibodies. DNA was stained with 4′, 6-diamidino-2-phenylindole (Sigma). Images were acquired with a Zeiss confocal microscope and analyzed with the LSM 510 software (Carl Zeiss).

Cell counting and statistical analysis

To count spiral ganglion cells at E12.5, ∼11 serial sections containing the entire cochlear duct were first stained with antibodies to ISL1. Then a total of 30 546 ISL1+ cells were counted. To count CVG neurons at E11.5, five to seven serial sections were co-labeled with ISL1 and pH3 and were imaged on a Zeiss confocal microscope. Since it is difficult to count CVG at E11.5, the areas of ISL1+ cells were measured morphometrically by using Abode Illustrator (Telegraphics) or ImageJ. Then pH3+ cells were counted. To quantify apoptotic cells, five or more serial sections spanning from the base to the middle part of the cochlear duct were immunolabeled with anti-SOX2 and anti-CASP3. High-quality images were obtained on Zeiss 510 META confocal microscope and were analyzed with the LSM 510 software. For each group, at least three animals were analyzed. Statistical analyses were performed by utilizing SPSS (v16.0). Two-tailed Student's *t*-test and Fisher's exact test were used to assess the statistical significance. $P \leq 0.05$ was considered statistically significant. Data represent mean ± SEM (standard error of the mean).

In situ hybridization

In situ hybridization was carried out as previously described (53). In brief, E13.5 embryos were fixed in 4% PFA in PBS at 4°C overnight, washed three times with PBS and cryoprotected in 30% sucrose in PBS. The heads were then embedded in OCT compound (TissueTek) and immediately frozen on dry ice. Twenty-micrometer cryosections were then subjected to *in situ* hybridization. Hybridization was conducted by using digoxigenin-labeled RNA probes. The following probes were used: *Bmp4* and *Fgf10*.

Whole mount immunohistochemistry

Whole mount immunohistochemistry was performed as previous described (53). Briefly, whole inner ear of E13.5 embryos was isolated under the dissecting microscope. The inner ear was then treated with collagenase (1 mg/ml) (Worthington) and neutral protease (1 mg/ml) (Worthington) for 8 min in cold HBSS (Invitrogen). The HBSS solution was replaced by DMEM/F12 (contained 5% FCS) and incubated for 30 min, and the entire cochlea was isolated under the dissecting microscope. The cochlea was fixed in 4% PFA in PBS for 1 h at 4°C, washed with three times PBS and subjected to immunohistochemistry. For immunostaining, the cochlea was permeabilized and blocked in PBS plus 0.1% Triton-X100, 0.03% saponin, 10% horse serum, incubated for 30 min at room temperature, then incubated with primary antibody (diluted in PBS plus 0.1% Triton-X100, 0.03% saponin, 3% horse serum, and 3% BSA) at 4°C overnight. In the next day, wash the cochlea in PBS for ∼8 h, and incubated with fluorescently labeled secondary antibody 4°C overnight. The following primary antibodies were used: SOX2 (Santa Cruz, 1:200) and $P27^{kip1}$ antibodies (BD Pharmingen, 1:200).

RNA-Sequencing (RNA-Seq)

The whole inner ear (includes otic epithelium plus surrounding mesenchyme) of E13.5 embryo mice was isolated under a dissecting microscope. To obtain adequate amount of total RNA, we pooled eight pairs of inner ears into one sample. Totally, two samples from wild-type and *Gata3-null* mice were collected. More detailed information about total RNA extraction, amplification, library construction, sequencing, and related analyses can be found in Supplementary material.

Real-time quantitative PCR

The whole inner ear of E13.5 embryo mice was isolated as described in RNA-Seq. To obtain adequate amount of total RNA, we combined eight pairs of inner ears into one sample.

Totally, three samples from wild-type and *Gata3-null* mice were collected. Total RNA extraction, cDNA synthesis and real-time PCR were performed as previously described (54). Briefly, total RNA was extracted using TRIzol reagent (Invitrogen) following the manufacturer's instructions. To remove the potential DNA contamination, we treated the RNA with DNase I (Fermentas). After DNase I digestion, 3 μg total RNA was used to synthesize cDNA by using oligo-$dT_{(20)}$ primers and Superscript III Reverse Transcriptase (Invitrogen). Quantitative PCR was performed by using the SYBR Green master mix and the Bio-Rad CFX Real-Time PCR Systems (BioRad). The specificity of product was ensured by melting curve analysis and agrose gel electrophoresis. The cDNA content of samples was normalized to the expression of *Actb* (β-actin), *Ubc* (ubiquitin C) and *Hsp90ab1* (Hsp90b1) genes as described previously (55). The analysis of quantitative PCR data was based on the ΔC_t values and fold change was determined by the $2^{-\Delta\Delta Ct}$ method. Real-time primers can be found in the Supplementary Material, Table S1.

SUPPLEMENTARY MATERIAL

Supplementary Material is available at *HMG* online.

ACKNOWLEDGEMENTS

We thank Amy Kiernan, Richard Libby, White Patricia and the member of Gan laboratory for their insightful discussions and technical assistance.

Conflict of Interest statement. None declared.

FUNDING

This work was supported by National Institute of Health grant DC008856, National Natural Science Foundation of China grant no. 81271006 and Hangzhou City Health Science Foundation grant no. 20120633B01.

REFERENCES

1. Anagnostopoulos, A.V. (2002) A compendium of mouse knockouts with inner ear defects. *Trends Genet.*, **18**, 499.
2. Bermingham, N.A., Hassan, B.A., Price, S.D., Vollrath, M.A., Ben-Arie, N., Eatock, R.A., Bellen, H.J., Lysakowski, A. and Zoghbi, H.Y. (1999) Math1: an essential gene for the generation of inner ear hair cells. *Science*, **284**, 1837–1841.
3. Kiernan, A.E., Pelling, A.L., Leung, K.K., Tang, A.S., Bell, D.M., Tease, C., Lovell-Badge, R., Steel, K.P. and Cheah, K.S. (2005) Sox2 is required for sensory organ development in the mammalian inner ear. *Nature*, **434**, 1031–1035.
4. Torres, M., Gomez-Pardo, E. and Gruss, P. (1996) Pax2 contributes to inner ear patterning and optic nerve trajectory. *Development*, **122**, 3381–3391.
5. Xiang, M., Gan, L., Li, D., Chen, Z.Y., Zhou, L., O'Malley, B.W. Jr, Klein, W. and Nathans, J. (1997) Essential role of POU-domain factor Brn-3c in auditory and vestibular hair cell development. *Proc. Natl Acad. Sci. USA*, **94**, 9445–9450.
6. Xiang, M., Maklad, A., Pirvola, U. and Fritzsch, B. (2003) Brn3c null mutant mice show long-term, incomplete retention of some afferent inner ear innervation. *BMC Neurosci.*, **4**, 2.
7. Chen, P., Johnson, J.E., Zoghbi, H.Y. and Segil, N. (2002) The role of Math1 in inner ear development: uncoupling the establishment of the sensory primordium from hair cell fate determination. *Development*, **129**, 2495–2505.
8. Kim, W.Y., Fritzsch, B., Serls, A., Bakel, L.A., Huang, E.J., Reichardt, L.F., Barth, D.S. and Lee, J.E. (2001) NeuroD-null mice are deaf due to a severe loss of the inner ear sensory neurons during development. *Development*, **128**, 417–426.
9. Puligilla, C., Dabdoub, A., Brenowitz, S.D. and Kelley, M.W. (2010) Sox2 induces neuronal formation in the developing mammalian cochlea. *J. Neurosci.*, **30**, 714–722.
10. Patient, R.K. and McGhee, J.D. (2002) The GATA family (vertebrates and invertebrates). *Curr. Opin. Genet. Dev.*, **12**, 416–422.
11. Van Esch, H., Groenen, P., Nesbit, M.A., Schuffenhauer, S., Lichtner, P., Vanderlinden, G., Harding, B., Beetz, R., Bilous, R.W., Holdaway, I. *et al.* (2000) GATA3 haplo-insufficiency causes human HDR syndrome. *Nature*, **406**, 419–422.
12. Van Esch, H. and Devriendt, K. (2001) Transcription factor GATA3 and the human HDR syndrome. *Cell. Mol. Life Sci.*, **58**, 1296–1300.
13. Grote, D., Souabni, A., Busslinger, M. and Bouchard, M. (2006) Pax 2/8-regulated Gata 3 expression is necessary for morphogenesis and guidance of the nephric duct in the developing kidney. *Development*, **133**, 53–61.
14. Grigorieva, I.V., Mirczuk, S., Gaynor, K.U., Nesbit, M.A., Grigorieva, E.F., Wei, Q., Ali, A., Fairclough, R.J., Stacey, J.M., Stechman, M.J. *et al.* (2010) Gata3-deficient mice develop parathyroid abnormalities due to dysregulation of the parathyroid-specific transcription factor Gcm2. *J. Clin. Invest.*, **120**, 2144–2155.
15. Rivolta, M.N. and Holley, M.C. (1998) GATA3 is downregulated during hair cell differentiation in the mouse cochlea. *J. Neurocytol.*, **27**, 637–647.
16. Karis, A., Pata, I., van Doorninck, J.H., Grosveld, F., de Zeeuw, C.I., de Caprona, D. and Fritzsch, B. (2001) Transcription factor GATA-3 alters pathway selection of olivocochlear neurons and affects morphogenesis of the ear. *J. Comp. Neurol.*, **429**, 615–630.
17. Lawoko-Kerali, G., Rivolta, M.N. and Holley, M. (2002) Expression of the transcription factors GATA3 and Pax2 during development of the mammalian inner ear. *J. Comp. Neurol.*, **442**, 378–391.
18. Rivolta, M.N., Halsall, A., Johnson, C.M., Tones, M.A. and Holley, M.C. (2002) Transcript profiling of functionally related groups of genes during conditional differentiation of a mammalian cochlear hair cell line. *Genome Res.*, **12**, 1091–1099.
19. Hawkins, R.D., Bashiardes, S., Helms, C.A., Hu, L., Saccone, N.L., Warchol, M.E. and Lovett, M. (2003) Gene expression differences in quiescent versus regenerating hair cells of avian sensory epithelia: implications for human hearing and balance disorders. *Hum. Mol. Genet.*, **12**, 1261–1272.
20. Lawoko-Kerali, G., Rivolta, M.N., Lawlor, P., Cacciabue-Rivolta, D.I., Langton-Hewer, C., van Doorninck, J.H. and Holley, M.C. (2004) GATA3 and NeuroD distinguish auditory and vestibular neurons during development of the mammalian inner ear. *Mech. Dev.*, **121**, 287–299.
21. van der Wees, J., van Looij, M.A., de Ruiter, M.M., Elias, H., van der Burg, H., Liem, S.S., Kurek, D., Engel, J.D., Karis, A., van Zanten, B.G. *et al.* (2004) Hearing loss following Gata3 haploinsufficiency is caused by cochlear disorder. *Neurobiol. Dis.*, **16**, 169–178.
22. Lillevali, K., Matilainen, T., Karis, A. and Salminen, M. (2004) Partially overlapping expression of Gata2 and Gata3 during inner ear development. *Dev. Dyn.*, **231**, 775–781.
23. van Looij, M.A., van der Burg, H., van der Giessen, R.S., de Ruiter, M.M., van der Wees, J., van Doorninck, J.H., De Zeeuw, C.I. and van Zanten, G.A. (2005) GATA3 haploinsufficiency causes a rapid deterioration of distortion product otoacoustic emissions (DPOAEs) in mice. *Neurobiol. Dis.*, **20**, 890–897.
24. Lillevali, K., Haugas, M., Matilainen, T., Pussinen, C., Karis, A. and Salminen, M. (2006) Gata3 is required for early morphogenesis and Fgf10 expression during otic development. *Mech. Dev.*, **123**, 415–429.
25. Lu, C.C., Appler, J.M., Houseman, E.A. and Goodrich, L.V. (2011) Developmental profiling of spiral ganglion neurons reveals insights into auditory circuit assembly. *J. Neurosci.*, **31**, 10903–10918.
26. Pandolfi, P.P., Roth, M.E., Karis, A., Leonard, M.W., Dzierzak, E., Grosveld, F.G., Engel, J.D. and Lindenbaum, M.H. (1995) Targeted disruption of the GATA3 gene causes severe abnormalities in the nervous system and in fetal liver haematopoiesis. *Nat. Genet.*, **11**, 40–44.
27. Haugas, M., Lillevali, K. and Salminen, M. (2012) Defects in sensory organ morphogenesis and generation of cochlear hair cells in Gata3-deficient mouse embryos. *Hear. Res.*, **283**, 151–161.
28. Kelley, M.W. (2006) Regulation of cell fate in the sensory epithelia of the inner ear. *Nat. Rev. Neurosci.*, **7**, 837–849.

29. Morsli, H., Choo, D., Ryan, A., Johnson, R. and Wu, D.K. (1998) Development of the mouse inner ear and origin of its sensory organs. *J. Neurosci.*, **18**, 3327–3335.
30. Radde-Gallwitz, K., Pan, L., Gan, L., Lin, X., Segil, N. and Chen, P. (2004) Expression of Islet1 marks the sensory and neuronal lineages in the mammalian inner ear. *J. Comp. Neurol.*, **477**, 412–421.
31. Ohyama, T. and Groves, A.K. (2004) Generation of Pax2-Cre mice by modification of a Pax2 bacterial artificial chromosome. *Genesis*, **38**, 195–199.
32. Ohyama, T., Basch, M.L., Mishina, Y., Lyons, K.M., Segil, N. and Groves, A.K. (2010) BMP signaling is necessary for patterning the sensory and nonsensory regions of the developing mammalian cochlea. *J. Neurosci.*, **30**, 15044–15051.
33. Dabdoub, A., Puligilla, C., Jones, J.M., Fritzsch, B., Cheah, K.S., Pevny, L.H. and Kelley, M.W. (2008) Sox2 signaling in prosensory domain specification and subsequent hair cell differentiation in the developing cochlea. *Proc. Natl Acad. Sci. USA*, **105**, 18396–18401.
34. Smith, R.J., Bale, J.F. Jr and White, K.R. (2005) Sensorineural hearing loss in children. *Lancet*, **365**, 879–890.
35. Muroya, K., Hasegawa, T., Ito, Y., Nagai, T., Isotani, H., Iwata, Y., Yamamoto, K., Fujimoto, S., Seishu, S., Fukushima, Y. *et al.* (2001) GATA3 abnormalities and the phenotypic spectrum of HDR syndrome. *J. Med. Genet.*, **38**, 374–380.
36. Fukami, M., Muroya, K., Miyake, T., Iso, M., Kato, F., Yokoi, H., Suzuki, Y., Tsubouchi, K., Nakagomi, Y., Kikuchi, N. *et al.* (2011) GATA3 abnormalities in six patients with HDR syndrome. *Endocr. J.*, **58**, 117–121.
37. Ralston, A., Cox, B.J., Nishioka, N., Sasaki, H., Chea, E., Rugg-Gunn, P., Guo, G., Robson, P., Draper, J.S. and Rossant, J. (2010) Gata3 regulates trophoblast development downstream of Tead4 and in parallel to Cdx2. *Development*, **137**, 395–403.
38. Economou, A., Datta, P., Georgiadis, V., Cadot, S., Frenz, D. and Maconochie, M. (2013) Gata3 directly regulates early inner ear expression of Fgf10. *Dev. Biol.*, **374**, 210–222.
39. Pirvola, U., Ylikoski, J., Trokovic, R., Hebert, J.M., McConnell, S.K. and Partanen, J. (2002) FGFR1 is required for the development of the auditory sensory epithelium. *Neuron*, **35**, 671–680.
40. Jacques, B.E., Montcouquiol, M.E., Layman, E.M., Lewandoski, M. and Kelley, M.W. (2007) Fgf8 induces pillar cell fate and regulates cellular patterning in the mammalian cochlea. *Development*, **134**, 3021–3029.
41. Hatch, E.P., Noyes, C.A., Wang, X., Wright, T.J. and Mansour, S.L. (2007) Fgf3 is required for dorsal patterning and morphogenesis of the inner ear epithelium. *Development*, **134**, 3615–3625.
42. Zelarayan, L.C., Vendrell, V., Alvarez, Y., Dominguez-Frutos, E., Theil, T., Alonso, M.T., Maconochie, M. and Schimmang, T. (2007) Differential requirements for FGF3, FGF8 and FGF10 during inner ear development. *Dev. Biol.*, **308**, 379–391.
43. Ladher, R.K., Wright, T.J., Moon, A.M., Mansour, S.L. and Schoenwolf, G.C. (2005) FGF8 initiates inner ear induction in chick and mouse. *Genes Dev.*, **19**, 603–613.
44. Alvarez, Y., Alonso, M.T., Vendrell, V., Zelarayan, L.C., Chamero, P., Theil, T., Bosl, M.R., Kato, S., Maconochie, M., Riethmacher, D. *et al.* (2003) Requirements for FGF3 and FGF10 during inner ear formation. *Development*, **130**, 6329–6338.
45. Wright, T.J. and Mansour, S.L. (2003) Fgf3 and Fgf10 are required for mouse otic placode induction. *Development*, **130**, 3379–3390.
46. Pauley, S., Wright, T.J., Pirvola, U., Ornitz, D., Beisel, K. and Fritzsch, B. (2003) Expression and function of FGF10 in mammalian inner ear development. *Dev. Dyn.*, **227**, 203–215.
47. Rusznak, Z. and Szucs, G. (2009) Spiral ganglion neurones: an overview of morphology, firing behaviour, ionic channels and function. *Pflugers Arch.*, **457**, 1303–1325.
48. Zilberstein, Y., Liberman, M.C. and Corfas, G. (2012) Inner hair cells are not required for survival of spiral ganglion neurons in the adult cochlea. *J. Neurosci.*, **32**, 405–410.
49. Tsarovina, K., Reiff, T., Stubbusch, J., Kurek, D., Grosveld, F.G., Parlato, R., Schutz, G. and Rohrer, H. (2010) The Gata3 transcription factor is required for the survival of embryonic and adult sympathetic neurons. *J. Neurosci.*, **30**, 10833–10843.
50. Martin, S.J., Lennon, S.V., Bonham, A.M. and Cotter, T.G. (1990) Induction of apoptosis (programmed cell death) in human leukemic HL-60 cells by inhibition of RNA or protein synthesis. *J. Immunol.*, **145**, 1859–1867.
51. George, S.H., Gertsenstein, M., Vintersten, K., Korets-Smith, E., Murphy, J., Stevens, M.E., Haigh, J.J. and Nagy, A. (2007) Developmental and adult phenotyping directly from mutant embryonic stem cells. *Proc. Natl Acad. Sci. USA*, **104**, 4455–4460.
52. Ding, Q., Chen, H., Xie, X., Libby, R.T., Tian, N. and Gan, L. (2009) BARHL2 differentially regulates the development of retinal amacrine and ganglion neurons. *J. Neurosci.*, **29**, 3992–4003.
53. Deng, M., Pan, L., Xie, X. and Gan, L. (2010) Requirement for Lmo4 in the vestibular morphogenesis of mouse inner ear. *Dev. Biol.*, **338**, 38–49.
54. Luo, X.J., Li, M., Huang, L., Nho, K., Deng, M., Chen, Q., Weinberger, D.R., Vasquez, A.A., Rijpkema, M., Mattay, V.S. *et al.*. (2012) The interleukin 3 gene (IL3) contributes to human brain volume variation by regulating proliferation and survival of neural progenitors. *PLoS ONE*, **7**, e50375.
55. Vandesompele, J., De Preter, K., Pattyn, F., Poppe, B., Van Roy, N., De Paepe, A. and Speleman, F. (2002) Accurate normalization of real-time quantitative RT-PCR data by geometric averaging of multiple internal control genes. *Genome Biol.*, **3**, RESEARCH0034.